Appl. Phys. A 55, 242–249 (1992)

Applied Physics A Solids and Surfaces

Analytic Construction of Magnetic Multipoles from Cylindric Permanent Magnets

V. Frerichs, W. G. Kaenders, and D. Meschede

Institut für Quantenoptik, Universität Hannover, Welfengarten 1, W-3000 Hannover, Fed. Rep. Germany
(Fax: +49-511/762-2211)

Received 23 December 1991/Accepted 7 May 1992

Abstract. We discuss an analytic method for the design of three-dimensional magnetic multipoles from permanent magnet materials. The concept is explicited with an idealized, continuously varying magnetization. The effect of segmentation for realistic implementations is discussed. As an example we present an open, experimentally accessible cylindric structure for a dipole and a quadrupole field with high purity. The fields are useful over several cm^3.

PACS: 07.55.+x, 85.70.Ec

The magnetic field strength generated from permanent magnet materials is invariant if all physical dimensions are scaled linearly. In contrast, the current density required by an equivalent solenoid system grows with the inverse of the dimension and hence leads to technical problems such as cooling efficiency etc. Permanent magnets offer furthermore compact structures and independence of utilities, and as a result may be competitive or even superior in terms of achievable field strength at small scales of order cm [1].

The construction of permanent magnet assemblies for the production of magnetic field configuration has much been facilitated since the arrival of rare earth materials (REM) with remanence $B_r > 1\,T$ and large coercitive forces [2]. REM-systems are particularly useful, since the fields of individual magnetic moments may be linearly superposed to a good approximation, which makes an analytical treatment possible.

The design of such systems, i.e. the distribution of magnetization, is determined by their application. Two-dimensional systems for accelerators and for synchrotron radiation sources have been studied in great detail both theoretically and experimentally [3, 4]. While those systems still operate at relatively large scale there is a growing interest for such systems at a more moderate scale also. Potential applications include magnets for nuclear magnetic resonance spectroscopy [5], Penning traps [6] for low energy charged particles and magnetic quadrupole traps [7] for neutral atoms. It is interesting to note that the cylindrical geometry that we will discuss is for instance fully compatible with a more recent design [8] of electrodes to produce an electric quadrupole field for a Penning trap. Hence these concepts may be easily combined. While Penning traps for precision measurements set stringent demands on field homogeneity, the sheer strength of a quadrupole field is of interest for the construction of a magnetic trap for neutral atoms. A two-dimensional variant of this method has already been demonstrated with permanent magnets [9].

We will introduce our concept by giving some simple arguments on how to arrange magnetized material in order to construct a certain magnetic field configuration. This reasoning will lead us to a general treatment, by which we will explore the experimentally interesting

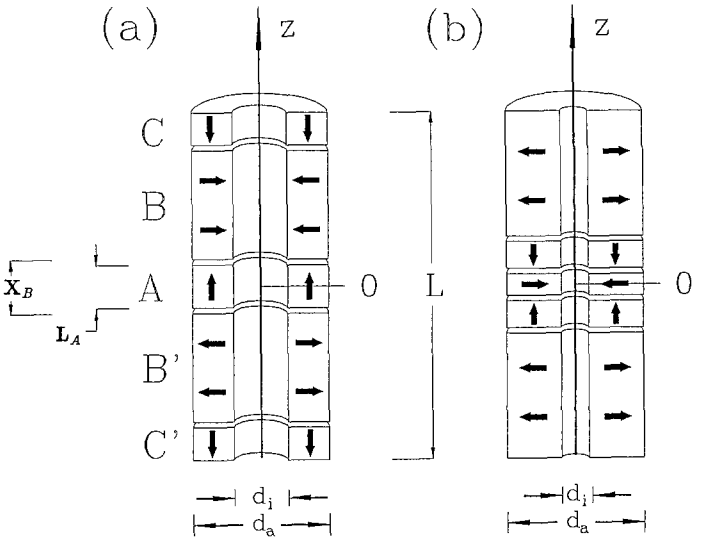

Fig. 1a, b. Construction of a magnetic dipole (**a**) and a magnetic quadrupole (**b**) from axially and radially magnetized cylindrical elements (not to scale). Multipoles are analyzed with respect to the origin at $z=0$. The convergence volume is a sphere centered at the origin and of diameter d_i

special case of open cylindrical structures (Fig. 1), which allow direct access to the field region of interest. Those components can be treated analytically, are relatively simple to build and allow furthermore a tuning reduction of imperfections. Simple special cases of our problem have been treated by other authors [5, 10].

1 Optimum Orientation of Magnetization

Since the superposition principle holds, one can consider any problem as a combination of the field or potentials of individual elementary dipoles **m**. For a given magnetic material one cannot vary the absolute value of magnetization, i.e. magnetic dipole moment per volume, but its orientation. Therefore, we begin by asking the question: What is the optimum orientation of a magnetic dipole at a particular position in space (Fig. 2a) as to contribute optimum strength to a given multipole moment of the field? We will restrict ourselves to problems of azimuthal symmetry which can be treated in the $z\varrho$-plane. We consider a thin ring (Fig. 2b) of radius ϱ and separation z from the origin, magnetized with linear magnetic moment density $\mathbf{m}=(m_0/2\pi\varrho)\cos\alpha\mathbf{e}_z+(m_0/2\pi\varrho)\sin\alpha\mathbf{e}_\varrho$ forming an angle α with the z axis. At the origin **m** gives rise to the well-known potential [11]

$$\Phi_m=-\left(\frac{\mu_0}{4\pi}\right)\int_0^{2\pi}\varrho\,d\phi\,\frac{\mathbf{m}\cdot(\varrho\mathbf{e}_\varrho+z\mathbf{e}_z)}{(\varrho^2+z^2)^{3/2}}$$
$$=-\left(\frac{\mu_0 m_0}{4\pi}\right)\frac{z\cos\alpha+\varrho\sin\alpha}{(\varrho^2+z^2)^{3/2}}. \tag{1}$$

Assume we are aiming at constructing a maximum strength magnetic field at the origin. Only its z-component B_z can be nonzero. As Φ_m only depends on the vector of separation of the origin and the source points, B_z may be expressed as the derivative of Φ_m with respect to the source, $B_z=\partial/\partial z\Phi_m$.

$$B_z=-\left(\frac{\mu_0 m_0}{4\pi}\right)\frac{1}{(\varrho^2+z^2)^{5/2}}$$
$$\cdot[(\varrho^2-2z^2)\cos\alpha-3\varrho z\sin\alpha], \tag{2}$$

and the angle of maximum contribution is found from

$$\tan\alpha=\frac{3\varrho z}{2z^2-\varrho^2}=\frac{3\sin 2\theta}{3\cos 2\theta+1}=-\frac{1}{2}\frac{P_2^1(\cos\theta)}{P_2^0(\cos\theta)}, \tag{3}$$

where P_ℓ^m denote associated Legendre polynomials. The dependence of α vs θ is shown in Fig. 3a.

Similar arguments may be used to construct a strong magnetic quadrupole. In order to compensate any magnetic dipole component at the origin we have to choose the z-magnetization antisymmetric in z and the ϱ-magnetization symmetric in z. The strength of the quadrupole is then determined from $\partial^2/\partial z^2\Phi_m$,

$$\frac{\partial^2}{\partial z^2}\Phi_m=-\left(\frac{\mu_0 m_0}{4\pi}\right)\frac{3}{(\varrho^2+z^2)^{7/2}}$$
$$\cdot[z(2z^2-3\varrho^2)\cos\alpha+\varrho(4z^2-\varrho^2)\sin\alpha] \tag{4}$$

which demands an optimum angle consistent with

$$\tan\alpha=\frac{\varrho(4z^2-\varrho^2)}{z(2z^2-3\varrho^2)}=-\frac{1}{3}\frac{P_3^1(\cos\theta)}{P_3^0(\cos\theta)}. \tag{5}$$

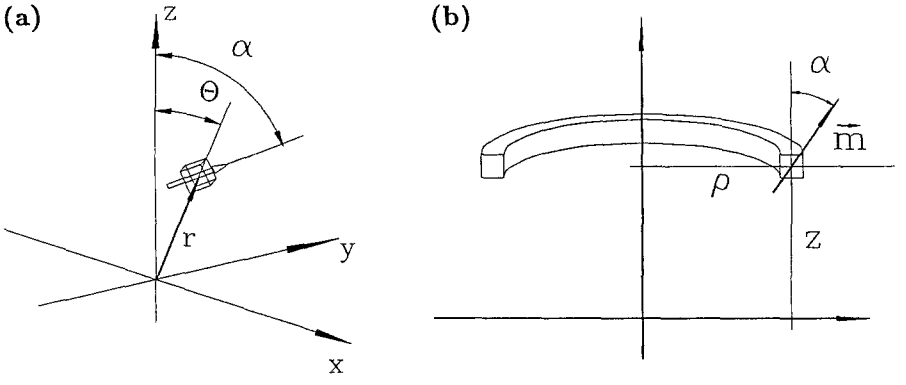

Fig. 2a, b. Geometry and coordinates of a magnetic dipole at a distance r from the origin (**a**), and thin magnetized ring at a distance $r=(\varrho^2+z^2)^{1/2}$ (**b**). The dipole axis is in the $r\theta$-plane and forms an angle α with the z-axis

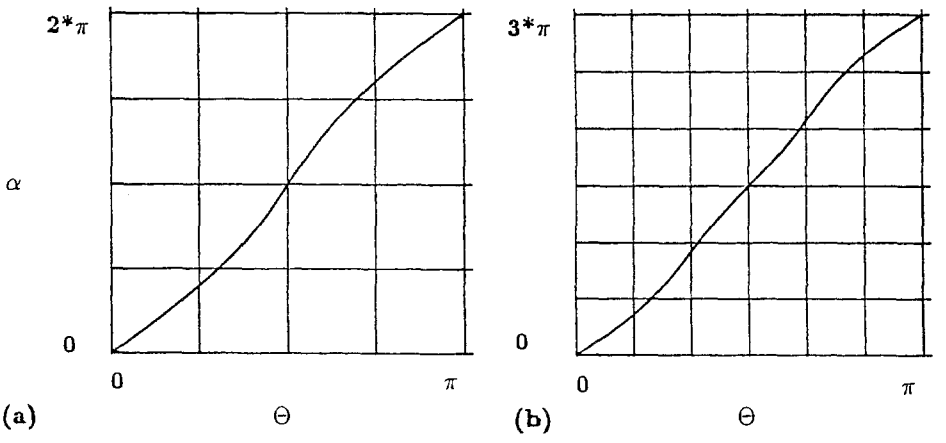

Fig. 3a, b. Angle α of the magnetization with the z-axis as a function of θ for maximum contribution to (**a**) dipole moment and (**b**) quadrupole moment

We show α vs θ in Fig. 3b. Note that our results are independent of geometry. The perturbation by other multipoles is, however, strongly determined by the specific choice of magnetic components. In the spirit of this introduction we will analyze cylindric components which allow immediate experimental access and hence are of preferential interest.

2 Three-Dimensional Multipoles

2.1 Idealized Continuously Varying Magnetization

We again restrict ourselves to multipoles of azimuthal symmetry. In spherical coordinates $r\theta\phi$ the magnetic potential of a pure axial multipole of order $2n$ can be written

$$\Phi_n(\mathbf{r}) = \Phi_0 r^n P_n(\cos\theta). \tag{6}$$

Obviously, the magnetization $\mathbf{M}$ required to create such a potential should reflect the azimuthal symmetry itself and hence is obtained by rotating the distribution in the xz-plane around the z-axis, i.e. it does not depend on ϕ and has no component parallel to $\mathbf{e}_\phi$. Furthermore, we will treat materials of constant magnetization $|\mathbf{M}(r',\theta'| = M_0$ only, which in spherical and cylinder coordinates is:

$$\begin{aligned}\mathbf{M} &= M_0\cos(\alpha-\theta')\mathbf{e}_{r'} + M_0\sin(\alpha-\theta')\mathbf{e}_{\theta'}\\ &= M_0\sin\alpha\mathbf{e}_{\varrho'} + M_0\cos\alpha\mathbf{e}_z.\end{aligned} \tag{7}$$

The angle α is a function of (ϱ', z') or $(r', \theta' = \arctan(\varrho'/z'))$ and describes the local angle between the magnetization $\mathbf{M}$ and the z-axis, $\mathbf{e}_z$ (Fig. 2). Following the arguments given in Sect. 1, the magnetic potential Φ_M is the sum of all dipole contributions within the magnetized volume $\mathcal{V}'$,

$$\Phi_M(\mathbf{r}) = -\left(\frac{\mu_0}{4\pi}\right)\int_{\mathcal{V}'}\frac{\mathbf{M}(\mathbf{r}')\cdot(\mathbf{r}'-\mathbf{r})}{|\mathbf{r}'-\mathbf{r}|^3}d^3r'. \tag{8}$$

We may rewrite (8),

$$\begin{aligned}\Phi_M(\mathbf{r}) &= -\left(\frac{\mu_0}{4\pi}\right)\nabla_r\int_{\mathcal{V}'}\frac{\mathbf{M}(\mathbf{r}')}{|\mathbf{r}'-\mathbf{r}|}d^3r'\\ &= \left(\frac{\mu_0}{4\pi}\right)\int_{\mathcal{V}'}\mathbf{M}(\mathbf{r}')\cdot\nabla_{r'}\frac{1}{|\mathbf{r}'-\mathbf{r}|}d^3r'.\end{aligned} \tag{9}$$

The scalar product $\mathbf{M}(\mathbf{r}')\cdot\nabla_{r'}$, which for arbitrary magnetization $M_{\varrho'}\mathbf{e}_{\varrho'} + M_{\phi'}\mathbf{e}_{\phi'} + M_{z'}\mathbf{e}_z$ reads

$$\mathbf{M}(\mathbf{r}')\cdot\nabla_{r'} = M_{\varrho'}\frac{\partial}{\partial\varrho'} + M_{z'}\frac{\partial}{\partial z'} + \frac{1}{\varrho'}M_{\phi'}\frac{\partial}{\partial\phi'}, \tag{10a}$$

does not depend on ϕ',

$$\mathbf{M}(\mathbf{r}')\cdot\nabla_{r'} = M_0\left\{\sin[\alpha(\theta')]\frac{\partial}{\partial\varrho'} + \cos[\alpha(\theta')]\frac{\partial}{\partial z'}\right\} \tag{10b}$$

in the case described by (7). If the magnetization is generally located outside the volume of interest ($r < r'$) we may use the well-known expansion [11]

$$\begin{aligned}\frac{1}{|\mathbf{r}'-\mathbf{r}|} = \sum_{\ell=0}^{\infty}\frac{r^\ell}{r'^{\ell+1}}\Bigg[&P_\ell(\cos\theta)P_\ell(\cos\theta')\\ &+2\sum_{m=1}^{\ell}\frac{(\ell-m)!}{(\ell+m)!}P_\ell^m(\cos\theta)P_\ell^m(\cos\theta')\cos m(\phi-\phi')\Bigg].\end{aligned} \tag{11}$$

We insert (10b) and (11) into (9) and carry out the ϕ'-integration immediately, which extinguishes the second term of the (11) and leaves us with the expected expansion in terms of Legendre polynomials,

$$\Phi_M = B_r\sum_{\ell=1}^{\infty}C_\ell r^\ell P_\ell(\cos\theta), \tag{12}$$

where M_0 has been replaced by the remanence field $B_r = \mu_0 M_0$.

Note that using (10a) instead of (10b), with $M_{\varrho'}$, $M_{z'}$, $M_{\phi'}$ expressed as Fourier series in ϕ', one obtains an expansion analogous to (12) valid inside a hollow magnet of arbitrarily chosen magnetization and shape. The second term of (11) then gives rise to terms proportional to $P_\ell^m(\cos\theta)\cos(m\phi)$ and $P_\ell^m(\cos\theta)\sin(m\phi)$. This result is used in Sect. 2.2.6 for calculating the perturbations arising in segmented magnets.

For a cylinder with radii ϱ_1 and ϱ_2 and with endcaps at z_1 and z_2, the coefficients in (12) are

$$\begin{aligned}C_\ell = \frac{1}{2}\int_{\varrho_1}^{\varrho_2}\varrho'd\varrho'\int_{z_1}^{z_2}dz'\\ \times\left\{\cos[\alpha(\varrho',z')]\frac{\partial}{\partial z'} + \sin[\alpha(\varrho',z')]\frac{\partial}{\partial\varrho'}\right\}\frac{P_\ell(\cos\theta')}{r'^{\ell+1}}.\end{aligned} \tag{13}$$

In particular, for $z_1 = -z_2$, all C_ℓ of even order ℓ vanish for $M_{\varrho'}(\varrho', z')$ an odd *and* $M_{z'}(\varrho', z')$ an even function in z'. For the opposite case all odd C_ℓ vanish. This generalizes the symmetry considerations in the introduction.

We can remove the differential operations in (13) exploiting the following recurrence relations,

$$\frac{\partial}{\partial z}\frac{P_\ell(\cos\theta)}{r^{\ell+1}} = -(\ell+1)\frac{P_{\ell+1}(\cos\theta)}{r^{\ell+2}}, \tag{14a}$$

$$\frac{\partial}{\partial\varrho}\frac{P_\ell(\cos\theta)}{r^{\ell+1}} = \frac{P_{\ell+1}^1}{r^{\ell+2}}, \tag{14b}$$

$$\frac{\partial}{\partial\varrho}\varrho\frac{\partial}{\partial\varrho}\frac{P_\ell(\cos\theta)}{r^{\ell+1}} = -\varrho\frac{\partial^2}{\partial z^2}\frac{P_\ell(\cos\theta)}{r^{\ell+1}}. \tag{14c}$$

For problems without cylindrical symmetry or with nonzero $M_{\phi'}$ one also needs

$$\begin{aligned}\frac{\partial}{\partial\varrho}\frac{P_\ell^m(\cos\theta)}{r^{\ell+1}} = \frac{1}{2r^{\ell+2}}\\ \times[P_{\ell+1}^{m+1}(\cos\theta) - (\ell-m+2)(\ell-m+1)P_{\ell+1}^{m-1}(\cos\theta)],\end{aligned} \tag{14d}$$

$$\frac{\partial}{\partial z}\frac{P_\ell^m(\cos\theta)}{r^{\ell+1}} = -\frac{1}{r^{\ell+2}}\{[P_{\ell+1}^m(\cos\theta)](\ell-m+1)\}. \tag{14e}$$

Equations (14d) and (14e) will not be used immediately, but they are required for treating, *e.g.* a cylindrical element made up from a finite number of segments (see Fig. 7 and Sect. 2.2.6 for this).

From (13), (14a), and (14b) we obtain

$$C_\ell = \frac{1}{2}\int_{\varrho_1}^{\varrho_2}\varrho' d\varrho' \int_{z_1}^{z_2} dz' \frac{1}{r'^{\ell+2}} \times \{-(\ell+1)\cos[\alpha(\varrho',z')]P_{\ell+1}(\cos\theta) + \sin[\alpha(\varrho',z')]P^1_{\ell+1}(\cos\theta')\}. \quad (15)$$

In agreement with special cases (3) and (5), we find from (15) that the angular variation of magnetization only depends on $\cos\theta' = z'/\varrho'$,

$$\tan\alpha(\theta) = -\frac{1}{\ell+1}\frac{P^1_{\ell+1}(\cos\theta')}{P_{\ell+1}(\cos\theta')} \quad (16)$$

for maximum possible contribution to a specific multipole or order 2ℓ. Clearly, the $1/r'^{\ell+2}$ factor in (15) makes spherical arrangements favorable. Cylindrical elements, however, are much simpler to construct and will be of dominating interest experimentally. If necessary, several cylinders may be stacked in order to take advantage of spherical structures.

In realistic situations we, furthermore, have to approximate the idealized continuous rotation of the magnetization by a finite number of homogeneously magnetized elements. Any azimuthal magnetization can be analyzed from a decomposition into radially and axially magnetized cylinder components. It is hence sufficient to restrict ourselves to the explicit discussion of these two special cases.

2.2 Magnetized Cylinders

We consider the two cases of axial magnetization ($\alpha = 0$ or π) and of radial magnetization ($\alpha = \mp\pi/2$) for cylindrical magnet components. Any other case may be treated as a superposition of these special cases.

From (16) it is clear that for a cylindrical assembly of elements that is to create an odd multipole, the conditions $M_{\varrho'}(\varrho', -z') = -M_{\varrho'}(\varrho', z')$ and $M_{z'}(\varrho', -z') = M_{z'}(\varrho', z')$ should hold everywhere, and vice versa for an even multipole. (In particular, the magnet's shape is always symmetrical under reflection on $z' = 0$). For calculating the multipole coefficients C_ℓ of such a configuration, it is convenient to express an element with radii ϱ_1 and ϱ_2 and with endcaps at z_1 and z_2 as the difference of the two z-semiinfinite shells extending from the lower bounds $z' = z_1$ and $z' = z_2$ to $z' = +\infty$. All one needs to know are the multipole coefficients of such z-semiinfinite magnets as functions of a variable lower bound z. These are denoted by C^0_ℓ if the magnetization points upwards (i.e. $\alpha = 0$) and by $C^{\pi/2}_\ell$ if the magnetization points radially outwards ($\alpha = \pi/2$), and are calculated now.

2.2.1 Axially Magnetized Cylinders. The z-integration of the first term in (13) is immediately carried out using (14a). For the z-semiinfinite magnet under consideration, extending from $z' = z$ to $z' = +\infty$ with $\alpha = 0$, we find with $r^2 = \varrho^2 + z^2$

$$C^0_\ell = \int_{\varrho_1}^{\varrho^2}\varrho d\varrho \int_z^\infty dz' \frac{d}{dz'}\frac{P_\ell(z'/r)}{r^{\ell+1}} = -\int_{\varrho_1}^{\varrho_2} d\varrho\varrho \frac{P_\ell(z/r)}{r^{\ell+1}} = -\int_{\varrho_1}^{\varrho_2}\frac{d\varrho\varrho}{\ell(\ell-1)}\frac{\partial^2}{\partial z^2}\frac{P_{\ell-2}\cos\theta}{r^{\ell-1}}. \quad (17)$$

A magnet of finite length may be composed of two such semiinfinite magnets with opposite magnetization.

With the help of (14b) and (14c), the coefficients can be given in closed form for $\ell \geqq 2$,

$$C^0_\ell = \frac{1}{2\ell(\ell-1)}\frac{\varrho P^1_{\ell-1}[z/(z^2+\varrho^2)^{1/2}]}{(z^2+\varrho^2)^{\ell/2}}\Bigg|_{\varrho_1}^{\varrho_2}. \quad (18)$$

The result for $\ell = 1$ is straightforwardly calculated from (13). The coefficients for $l = 1$ to 6 are:

$$C^0_1 = \frac{1}{2}\frac{z}{(\varrho^2+z^2)^{1/2}}\Bigg|_{\varrho_1}^{\varrho_2}, \quad (19a)$$

$$C^0_2 = -\frac{1}{4}\frac{\varrho^2}{(\varrho^2+z^2)^{3/2}}\Bigg|_{\varrho_1}^{\varrho_2}, \quad (19b)$$

$$C^0_3 = -\frac{1}{4}\frac{z\varrho^2}{(\varrho^2+z^2)^{5/2}}\Bigg|_{\varrho_1}^{\varrho_2}, \quad (19c)$$

$$C^0_4 = -\frac{1}{16}\frac{\varrho^2(6z^2-\varrho^2)}{(\varrho^2+z^2)^{7/2}}\Bigg|_{\varrho_1}^{\varrho_2}, \quad (19d)$$

$$C^0_5 = -\frac{1}{16}\frac{z\varrho^2(6z^2-3\varrho^2)}{(\varrho^2+z^2)^{9/2}}\Bigg|_{\varrho_1}^{\varrho_2}, \quad (19e)$$

$$C^0_6 = -\frac{1}{32}\frac{\varrho^2(10z^4-12z^2\varrho^2+\varrho^4)}{(\varrho^2+z^2)^{11/2}}\Bigg|_{\varrho_1}^{\varrho_2}. \quad (19f)$$

2.2.2 Radially Magnetized Cylinders. In this case ($\alpha = \pi/2$) only the second term in (13) survives. Incorporating again relation (14b) we find

$$C^{\pi/2}_\ell = \frac{1}{2}\int_{\varrho_1}^{\varrho_2} d\varrho\varrho \int_z^\infty dz' \frac{P^1_{\ell+1}(z'/r)}{r^{\ell+2}} = \frac{1}{2}\int_{\varrho_1}^{\varrho_2} d\varrho\varrho \frac{\partial}{\partial\varrho}\frac{1}{\ell}\frac{P_{\ell-1}(z/r)}{r^\ell}, \quad (20)$$

which by partial integration yields

$$C^{\pi/2}_\ell = \frac{1}{2\ell}\left[\frac{\varrho P_{\ell-1}(z/r)}{r^\ell}\Bigg|_{\varrho_1}^{\varrho_2} - \int_{\varrho_1}^{\varrho_2} d\varrho\frac{P_{\ell-1}(z/r)}{r^\ell}\right]. \quad (21)$$

Integration of (21) is somewhat tedious, but the final result for $\ell \geqq 2$ is

$$C^{\pi/2}_\ell = \frac{\varrho}{2\ell}\left[\frac{P_{\ell-1}(z/r)}{r^\ell} - \frac{1}{\ell-1}\sum_{k=0}^{\ell-2}\left(\frac{z}{r}\right)^{k+1}\frac{P_k(z/r)}{z^\ell}\right]\Bigg|_{\varrho_1}^{\varrho_2}. \quad (22)$$

Again $C^{\pi/2}_1$ is found by direct integration. Similar to the case $\alpha = 0$ we write the first six coefficients

$$C^{\pi/2}_1 = \frac{1}{2}\left(\frac{\varrho}{(\varrho^2+z^2)^{1/2}} - \ln[\varrho + (\varrho^2+z^2)^{1/2}]\right)\Bigg|_{\varrho_1}^{\varrho_2}, \quad (23a)$$

$$C^{\pi/2}_2 = -\frac{1}{4}\frac{\varrho^3}{z(\varrho^2+z^2)^{3/2}}\Bigg|_{\varrho_1}^{\varrho_2}, \quad (23b)$$

$$C^{\pi/2}_3 = -\frac{1}{12}\frac{\varrho^3(\varrho^2+4z^2)}{z^2(\varrho^2+z^2)^{5/2}}\Bigg|_{\varrho_1}^{\varrho_2}, \quad (23c)$$

$$C^{\pi/2}_4 = -\frac{1}{48}\frac{\varrho^3(2\varrho^4+7\varrho^2z^2+20z^4)}{z^3(\varrho^2+z^2)^{7/2}}\Bigg|_{\varrho_1}^{\varrho_2}, \quad (23d)$$

$$C^{\pi/2}_5 = -\frac{1}{80}\frac{\varrho^3(2\varrho^6+9\varrho^4z^2+12\varrho^2z^4+40z^6)}{z^4(\varrho^2+z^2)^{9/2}}\Bigg|_{\varrho_1}^{\varrho_2}, \quad (23e)$$

$$C_6^{\pi/2} = -\frac{1}{480} \times \frac{\varrho^3(10\varrho^8 + 44\varrho^6 z^2 + 99\varrho^4 z^4 + 28\varrho^2 z^6 + 280 z^8)}{z^5(\varrho^2+z^2)^{11/2}}\Bigg|_{\varrho_1}^{\varrho_2}. \quad (23f)$$

Equations (23) seem to diverge at $z=0$. The divergent part, though, is independent of ϱ and therefore cancels out, which is seen for $\ell \geqq 2$, e.g. by using the convenient recurrence relation (arbitrary fixed α)

$$C_{\ell+1}^{\alpha} = -\frac{1}{\ell+1}\frac{\partial}{\partial z} C_{\ell}^{\alpha} \quad (24)$$

with the Taylor series expansion of (23b) to obtain:

$\ell > 1$, even

$$C_{\ell}^{\pi/2} = \frac{(-1)^{(\ell-2)/2}}{2\varrho^{\ell-1}} \frac{(\ell+1)!!}{\ell!!\ell} \left(\frac{z}{\varrho}\right)\Bigg|_{\varrho_1}^{\varrho_2}; \quad (25a)$$

$\ell > 1$, odd

$$C_{\ell}^{\pi/2} = \frac{(-1)^{(\ell-1)/2}}{2\varrho^{\ell-1}} \frac{\ell!!}{\ell(\ell-1)(\ell-1)!!} \times \left\{1 - \frac{(\ell+2)\ell(\ell-1)}{2(\ell+1)}\left(\frac{z}{\varrho}\right)^2\right\}\Bigg|_{\varrho_1}^{\varrho_2}. \quad (25b)$$

For $\ell = 1$

$$C_1^{\pi/2} = -\frac{\ln\varrho}{2} - \frac{3z^2}{8\varrho^2}\Bigg|_{\varrho_1}^{\varrho_2} \quad (25c)$$

is found.

2.2.3 Properties of the C-Coefficients. The axial case $\alpha = 0$ and the radial case $\alpha = \pi/2$ are interrelated by

$$C_{\ell}^{\pi/2} = (\ell+1)\int_{\varrho_1}^{\varrho_2} d\varrho \chi_{\ell+1}^0, \quad (26)$$

where $\chi_{\ell+1}^0$ stands for the indefinite integral in ϱ corresponding to the definite integral $C_{\ell}^0(z)$ given in (18).

The symmetry properties of multipole coefficients (18) and (19) are given by $C_{\ell}^0(z) = (-1)^{\ell} C_{\ell}^0(-z)$, and for (22) and (23) are $C_{\ell}^{\pi/2}(z) = -(-1)^{\ell} C_{\ell}^{\pi/2}(-z)$. An odd multipole, such as the dipole of Fig. 1a, requires an array of cylindric magnet elements symmetric in the z-component and antisymmetric in the ϱ-component of magnetization. For an even multipole, for instance the quadrupole of Fig. 1b, the magnetization of elements is chosen antisymmetric in z and symmetric in ϱ.

2.2.4 Example: Construction of Dipoles and Quadrupoles. From (24) we conclude that the contribution of a thin, magnetized disc at location z and of thickness Δz to a given multipole of order $n = 2\ell$ at the origin is given by $dB_z = -(\ell+1)C_{\ell+1}^{\alpha} dz$. As an illustration we show in Fig. 4a the contribution of axially and radially magnetized discs to a magnetic dipole, i.e. C_2^0 and $C_2^{\pi/2}$, where we have chosen experimentally reasonable dimensions for the inner and outer diameter $d_i = 20$ mm and $d_a = 50$ mm of the cylinder. At each separation z we are free to select an optimum direction of magnetization for maximum contribution. According to Fig. 4a, the innermost cylinder A should be axially magnetized and 8 mm long, followed by two oppositely magnetized radial components B and B' of length 27.5 mm, and then axial components C and C' again oriented oppositely to the central one. The total dipole strength at the origin is given by the integral over the maximum C_2^{α} coefficients. This integral, $B_z(0) = -2B_r \int_0^{L/2} \max_{\{\alpha\}}(2|C_2^{\alpha}(z)|)dz$, is presented in Fig. 4b as a function of $L/2$, the total half length of the cylinder with optimum orientation of the magnetization. We note that in the central part of the system described within the linear approximation field strengths of the order of the remanence field B_r are obtained in a volume of a few cm^3. B_r may exceed 1.3 T for suitable materials such as NdFeB [2].

The maximum field strength is theoretically limited only by the ratio of the geometric dimensions. For large

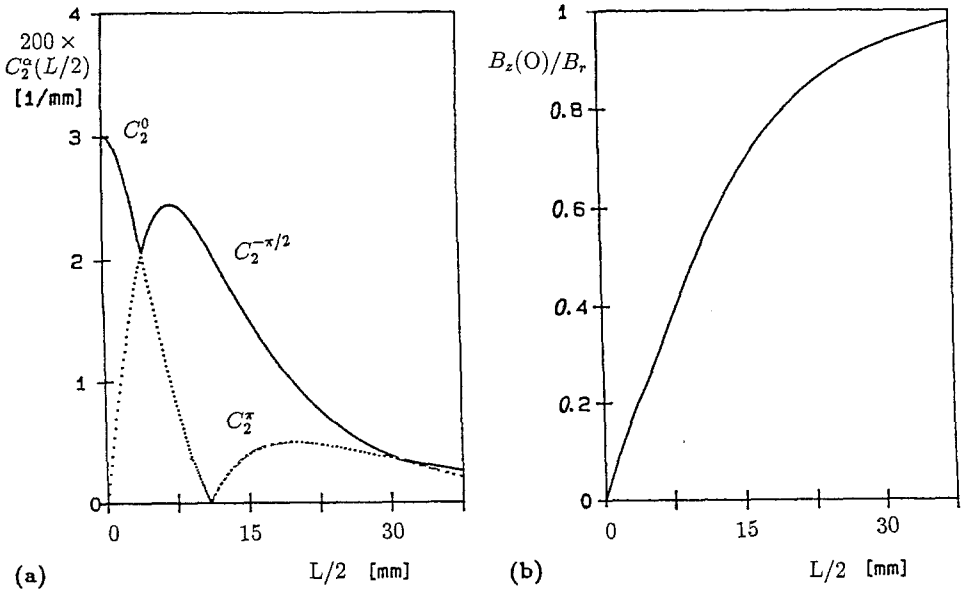

Fig. 4a, b. Construction of a magnetic dipole $D_i = 20$ mm, $D_a = 50$ mm. **(a)** Contribution of a thin disc situated at $z = L/2$ to the dipole field strength at the origin, $dB_z(0) = 2C_2^{\alpha}B_r dz$. (·····) – contribution of individual axial ($\alpha = 0$ or π) and radial ($\alpha = \pm\pi/2$) magnetization. Maximum contribution enhanced by (——). **(b)** Dipole field strength from pairs of discs at $\pm z$: $B_z(0)/B_r$ as a function of $L/2$, $B_z(0)/B_r = 2\int_0^{L/2} \max_{\{\alpha\}}[2C_2^{\alpha}(z)]dz$

outer diameters ($\varrho_2 \gg \varrho_1$) and very long ($L/2 \gg \varrho_1$) radially magnetized cylinders we reproduce the known result [10] that the field strength near the origin diverges like

$$B_z \simeq B_r \ln\left(\frac{\varrho_2}{\varrho_1}\right). \tag{27}$$

In this case very large demagnetizing fields exceeding the coercitive force will occur and hence limit any realistic system.

Another case of interest [7] is the construction of a magnetic quadrupole. Following the reasoning for the dipole we have to choose the magnetization from the maximum value of the C_3^α coefficients, which are given in Fig. 5a. The gradient of the magnetic field strength in the z-direction as derived from the quadrupole coefficient of such a realistic system is given in Fig. 5b and may overcome 1 T/cm. It is, of course, interesting to estimate the maximum field gradient possible, which can be achieved by choosing the magnetization according to (7). For an infinitely long cylindric structure of inner and outer radii ϱ_1 and ϱ_2, we find a maximum coefficient $|C_2|$

$$|C_2| \leqq \frac{1}{2}\left| \int_{-\infty}^{\infty} dz \int_{\varrho_i}^{\varrho_a} \varrho d\varrho \frac{1}{r^4} \{[3P_3^0(z/r)]^2 + [P_3^1(z/r)]^2\}^{1/2} \right|$$
$$= 1.63 \frac{3}{4}\left(\frac{1}{\varrho_i} - \frac{1}{\varrho_a}\right). \tag{28}$$

From (28) we conclude that the maximum field gradient to be expected is approximately $2.4 B_r/\varrho_1$. Clearly, at the aperture ϱ_1 of the cylinder the radial field strength at $z=0$ exceeds the remanence strength by a factor 1.2. Inside the material strong demagnetizing fields may occur and hence the application of materials with high coercitive forces is mandatory.

2.2.5 Compensation of Higher Order Multipoles. Not only the achievable multipole strength is of interest but also its purity or homogeneity. For the dipole construction of Fig. 1 and Fig. 4 we demonstrate one of several possible strategies to compensate higher order multipoles based on the alignment of cylinder segments only. Obviously, these efforts may be supplemented by external low current shim coils which we will not consider here, however.

Due to symmetry only odd multipole moments do exist in the cylindric magnetic dipole and hence the C_3^α coefficients are to be compensated. In our construction (Fig. 1) the dipole ($\ell=1$) contributions of the inner three elements A, B, B' are essential only, and we neglect the influence of C and C'. The $\ell=3$ contribution of A is $-2C_3^0(L_A/2)$ as a function of its length L_A. The two radial cylinders B and B' are chosen somewhat longer than in our example with 45 mm length, their $\ell=3$ contribution is $-2[C_3^{\pi/2}(X_B/2) - C_3^{\pi/2}(X_B/2 + 45\text{ mm})]$ as a function of their separation X_B. From Fig. 6 it is seen that the sum is zero for several pairs (L_A; X_B). As an example, leaving out the innermost part of element A, i.e. splitting A into two elements extending from $z = \pm 2.7$ mm to $L_A/2 = \pm 7.1\text{ mm} = X_B/2$ yields 80% of the optimized field strength while the $\ell=3$ contributions vanish (see Fig. 6). The configuration is easily tunable by changing the separation of its two halves to a value differing from 5.4 mm. Not only the systematic effects described in this paragraph but also contributions due to imperfections such as variations in the direction of magnetization may be compensated in this way.

The leading term in the multipole expansion is now C_5 which is of order $10^{-2}/\text{cm}^4$, resulting in a dipole field inhomogeneity of order 10^{-3} within half the convergence radius, or a volume of about 1 cm^3 in our example.

2.2.6 Perturbations due to Radial Segmentation. The radially magnetized cylinders as described in Sect. 2.2.2 cannot in general be manufactured with continuously varying magnetization. Instead they will typically be assembled from N identical segments. The influence of this segmentation can be estimated from an azimuthal Fourier analysis of the magnetization that originally led us to neglect terms with $m>1$ in (11). First, the effective magnetization, i.e. the average radial magnetization

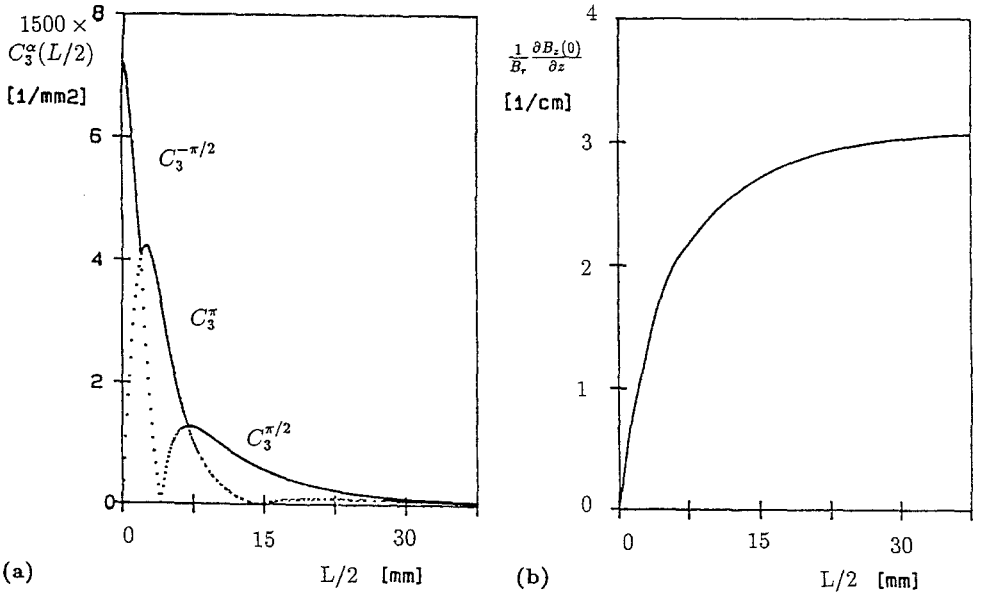

Fig. 5a, b. Construction of a magnetic quadrupole $D_i = 10$ mm, $D_a = 50$ mm. (**a**) Contribution of a thin disc situated at $z = L/2$ to the field gradient at the origin, $d(dB_z(0)/dz) = 6C_3^\alpha B_r dz$. (· · · ·) – contribution of individual axial ($\alpha = 0$ or π) and radial ($\alpha = \pm\pi/2$) magnetization. Maximum contribution enhanced by (——). (**b**) Field gradient $dB_z(0)/dz$ from pairs of thin discs at $\pm z$ as a function of $L/2$, $B_z = 2B_r = 2\int_0^{L/2} \max_{\{\alpha\}}[6C_3^\alpha] dz$

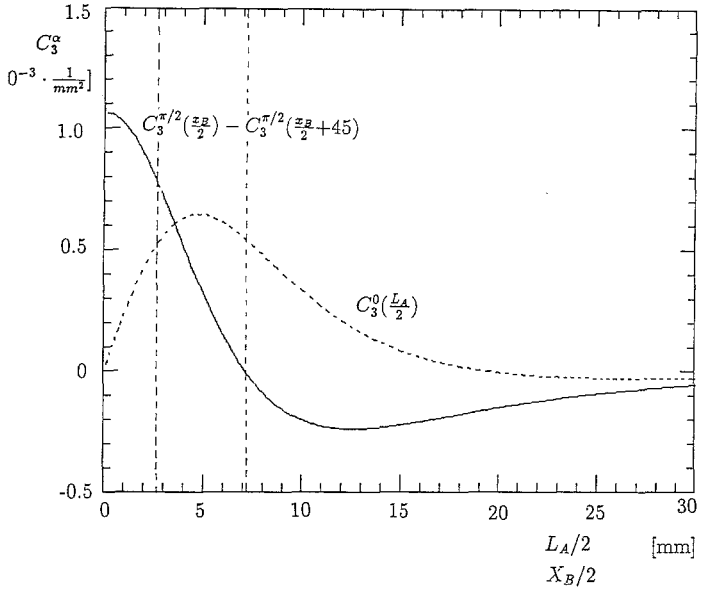

Fig. 6. Compensation of third order perturbation for a magnetic dipole. Dotted curve: C_3^0 as a function of half length $L_A/2$ (see Fig. 1a). Solid curve: $C_3^{\pi/2}$ as function of $X_B/2$, half separation of B and B' in Fig. 1a with fixed length of $B, B' = 45$ mm. Leaving out the part of A extending from $L_A/2 = 0$ to left vertical line and changing magnetization directions ($A \rightarrow B$) at right vertical line yields a tunable magnet with zero third order (hexapole) field

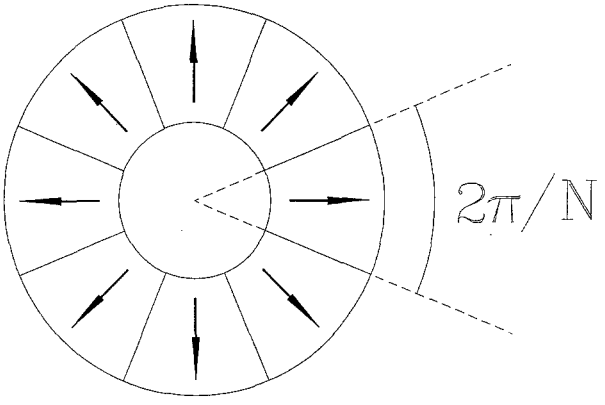

Fig. 7. Segmentation of radially magnetized cylinders

$\langle M_r \rangle$, will be reduced, and second, a perturbation of multipole orders $2N$ and higher is introduced.

The reduction of magnetization may straightforwardly be estimated from (Fig. 7)

$$\frac{\langle M_r \rangle}{M_0} = \frac{N}{2\pi} \int_{-\pi/N}^{\pi/N} \cos\phi d\phi = \frac{\sin(\pi/N)}{\pi/N}, \tag{29}$$

which gives $\langle M_r \rangle / M_0 = 97\%$ for $N = 8$ and 99% for $N = 12$. By the method outlined in Sect. 2.1 and using (14d) and (14e), we find that the leading perturbation varies as $r^N[C_{N\varrho}\cos(N\phi) + C_{N\phi}\sin(N\phi)]$ with coefficients $C_{N\varrho}$ and $C_{N\phi}$. After a lengthy calculation not reproduced here, we find that the magnitude of these does not exceed the $\frac{1}{N!}$th part of C_N^α, the fundamental coefficients of (18) and (22).

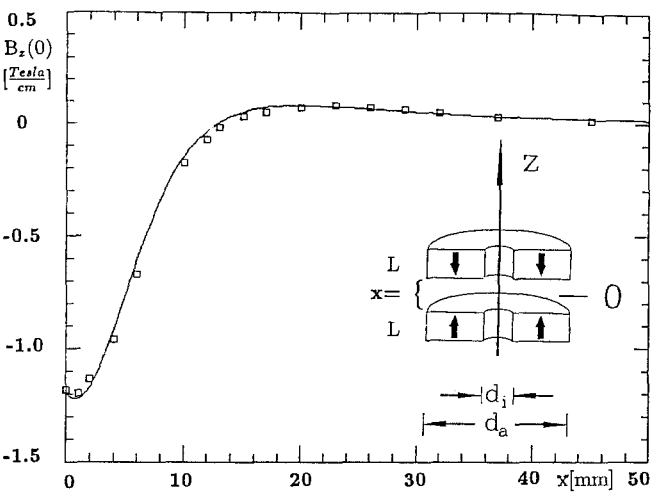

Fig. 8. Field gradient dB/dz ($z = 0$) of the rings shown in the inset vs separation x. (——) – calculation from (19b); □ – experiment. $B_r = 1.05$ T; $d_i = 9.4$ mm; $d_a = 19.4$ mm; $L = 5.0$ mm

3 Experimental Results for a Simple System

In order to demonstrate experimentally the validity of our calculations on real magnetic systems we used axially magnetized cylindrical rings designed for optical isolators, which were readily available in the laboratory. We assembled simple dipoles and quadrupoles with variable lengths and distances. An electronic integrator and a Hall probe were employed to measure magnetic moments and two- or three-dimensional magnetic field distributions.

Within a few percent predictions by our analytic treatment could be proven for various situations. As a simple example we give the quadrupole field gradient (Fig. 8) on the symmetry axis of two rings ($\varrho_1 = 4.7$ mm, $\varrho_2 = 9.7$ mm, $B_r = 1.0$ T) as a function of their separation x. We also tested the validity of linear superposition for the material used. We found the superposition principle to hold to a very good approximation even in this extreme case.

Combinations of cylindrical magnets optimized for maximum field strength or steep gradients with high purity are currently under construction. Results of this experiment will be the subject of a later report.

4 Conclusions

We have analytically calculated the magnetic field of cylindrical permanent magnets. From our calculation we can derive optimum conditions for the construction of strong magnetic multipoles with high purity. The cylindric structures are openly accessible, and the magnetic fields should be useful over several cm^3 under realistic conditions. A preliminary measurement showed good agreement with the calculated field distribution.

Acknowledgements. We would like to thank F. Schroeder and T. Müller-Wirts for technical assistance with the measurements. We, furthermore, acknowledge stimulating discussions with K. Halbach on our topic.

References

1. K. Halbach: Nucl. Instr. Meth. **169**, 1 (1980); Nucl. Instr. Meth. **198**, 213 (1982)
2. See. for example, *Seltene-Erd-Dauermagetwerkstoffe:* Catalogue, Vacuum Schmelze, Hanau, Germany (1988); *Dauermagnetische Werkstoffe und Bauteile:* Catalogue, Krupp Widia, Essen, Germany (1989); *Die Welt des Magnetismus:* Catalogue, IBS Magnet, Berlin, Germany (1990)
3. K. Halbach: Nucl. Instr. Meth. **187**, 109 (1981)
4. R.L. Gluckstern, R.F. Holsinger: Nucl. Instr. Meth. **187**, 119 (1981)
   W. Gudat, J. Pflüger, J. Chatzipetros, W. Peatman: Nucl. Instr. Meth. **246**, 50 (1986)
   W. Gudat, J. Pflüger: Z. Phys. B **61**, 483 (1985)
5. H.A. Leupold, E. Potenziani II: IEEE Trans. Magn. **23** (5), 3628 (1987)
   M.G. Abele, H.A. Leupold: J. Appl. Phys. **64**, 5988 (1988)
   H.A. Leupold, E. Potenziani, M.G. Abele: J. Appl. Phys. **64**, 5994 (1988)
   M.G. Abele: IEEE Trans. Magn. **26** (5), 1665 (1990)
6. L.S. Brown, G. Gabrielse: Rev. Mod. Phys. **58**, 233 (1986); 240 (1985)
7. A.L. Migdall, J. Prodan, W. Phillips, T. Bergeman, H. Metcalf: Phys. Rev. Lett. **54**, 2596 (1985)
   T. Bergeman, G. Erez, H. Metcalf: Phys. Rev. A **35**, 1535 (1987)
   T. Bergeman, P. McNicholl, J. Kycia, H. Metcalf, N. Balazs: J. Opt. Soc. Am. B **6**, 2249 (1989)
8. G. Gabrielse, F.C. Mackintosh: J. Mass Spectrom. **57**, 1 (1984)
   G. Gabrielse, L. Haarsma, S.L. Rolston: J. Mass Spectrom. **88**, 319 (1989)
9. J. Nellessen, J. Werner, W. Ertmer: Opt. Commun. **78**, 300 (1990)
10. Xu Quing: Nucl. Instr. Meth. Phys. Res. A **253**, 173 (1987)
    L. Mao-san, C. Ren-huai, W. Wen-tai, L. Shu-zhen: Phys. Energ. Fortis Phys. Nucl. **5**, 452 (1981) (in Chinese)
11. J.D. Jackson: *Classical Electrodynamics* (Wiley, New York 1975)